Supporting Information

The Quest for Simplicity - Remarks on the Free-Approach Models

Authors: Łukasz Jaremko*[,1,2], Mariusz Jaremko[1], Michał Nowakowski[3], Andrzej Ejchart[4]

[1] *Max Planck Institute for Biophysical Chemistry, Department for NMR-based Structural Biology, Am Fassberg 11, 37077 Göttingen, Germany, e-mail: jaremko@gmail.com*

[2] *Deutsches Zentrum für Neurodegenerative Erkrankungen (DZNE), Am Fassberg 11, 37077 Göttingen, Germany*

[3] *Centre of New Technologies, University of Warsaw, Banacha 2C, 02-097 Warsaw, Poland*

[4] *Institute of Biochemistry and Biophysics, Polish Academy of Sciences, Pawinskiego 5A, 02-106 Warsaw, Poland.*

TABLE OF CONTENTS

Basic equations for spin relaxation parameters

Two relaxation mechanisms have to be taken into account for the nuclear spin relaxation of amide nitrogens in proteins: the chemical shift anisotropy of a nitrogen nucleus and the dipolar interaction between a nitrogen and the hydrogen directly bound to it. Providing that interference between these two mechanisms and $^{1}H/^{15}N$ cross-relaxation are suppressed by appropriate design of pulse sequences[1,2] longitudinal (R_1) and transverse (R_2) relaxation rates are given as

$$R_1 = R_{1,DD} + R_{1,CSA} \tag{S1}$$

$$R_2 = R_{2,DD} + R_{2,CSA} + R_{ex} \tag{S2}$$

Additional conformational term R_{ex} is briefly discussed later (vide infra).

Rates due to dipolar and chemical shift anisotropy mechanisms are expressed in terms of spectral density functions[3]

$$R_{1,DD} = \frac{1}{4} D^2 [J(\omega_H - \omega_N) + 3J(\omega_N) + 6J(\omega_H + \omega_N)] \tag{S3}$$

$$R_{1,CSA} = \frac{1}{3} C^2 J(\omega_N) \tag{S4}$$

$$R_{2,DD} = \frac{1}{8} D^2 [4J(0) + J(\omega_H - \omega_N) + 3J(\omega_N) + 6J(\omega_H + \omega_N) + 6J(\omega_H)] \tag{S5}$$

$$R_{2,CSA} = \frac{1}{18} C^2 [4J(0) + 3J(\omega_N)] \tag{S6}$$

Third frequently measured relaxation parameter, nuclear Overhauser effect is given by

$$NOE = 1 + \frac{\gamma_H}{\gamma_N} \frac{\sigma}{R_1} \tag{S7}$$

where cross-relaxation rate is

$$\sigma = \frac{1}{4} D^2 [6J(\omega_H + \omega_N) - J(\omega_H - \omega_N)]$$

Appropriate amplitudes of dipolar and chemical shift anisotropy mechanisms are given by

$$D = -\frac{\mu_0}{4\pi} \gamma_H \gamma_N \hbar \left\langle r_{NH}^{-3} \right\rangle \tag{S8}$$

$$C = \gamma_N B_0 \Delta\sigma = \omega_N \Delta\sigma \tag{S9}$$

where $\left\langle r_{NH}^{-3} \right\rangle$ is vibrationally averaged N–H distance, $\Delta\sigma$ is anisotropy of axially symmetric ^{15}N shielding tensor, B_0 is external magnetic flux density, and other symbols have their usual meaning.

The additional term R_{ex} takes into account the conformational exchange contribution to R_2 resulting from processes in the micro- to millisecond time scale often referred to as chemical exchange effects[4]. Such processes, slower than the molecular tumbling, but fast enough to average chemical shifts, can influence transverse relaxation rates determined using the CPMG method[5,6]. The R_{ex} contribution to the transverse relaxation rate is proportional to the square of the chemical shift difference between exchanging states, $\Delta\delta$, and to ω_N, the Larmor frequency. It should be pointed out that the conformational exchange mechanism can affect the apparent transverse relaxation rate only if $\Delta\delta \neq 0$.

Anisotropy of rotational diffusion

Initially, spectral density functions in the formulation of model-free approaches described isotropic overall molecular tumbling characterized by correlation time τ_R. Even small degree of overall motional anisotropy usually modifies values of relaxation parameters. Such anisotropy has to be taken into account to avoid determination of false parameters of internal motion(s).

Therefore, model-free approach spectral density functions are combined with spectral density function describing molecule undergoing anisotropic overall tumbling. The latter comprises five terms and is given as[7]

$$J(\omega) = \sum_{i=1}^{5} A_i \frac{\tau_i}{1+(\omega\tau_i)^2} \qquad \text{(S10)}$$

Correlation times τ_i are expressed by principal components of rotational diffusion tensor D_k: $\tau_1 = (4D_1+D_2+D_3)^{-1}$, $\tau_2 = (D_1+4D_2+D_3)^{-1}$, $\tau_3 = (D_1+D_2+4D_3)^{-1}$, $\tau_4 = 6[D+(D^2-L^2)^{1/2}]^{-1}$, and $\tau_5 = 6[D-(D^2-L^2)^{1/2}]^{-1}$, where $D = (D_1+D_2+D_3)/3$ and $L^2 = (D_1D_2+D_2D_3+D_3D_1)/3$.

Directional factors A_i describe orientation of relaxation vector in the molecule fixed coordinate system in terms of direction cosines l, m, n: $A_1 = 3m^2n^2$, $A_2 = 3l^2n^2$, $A_3 = 3m^2l^2$, $A_4 = (d-e)/2$, $A_5 = (d+e)/2$, where

$d = 0.5[3(l^4+m^4+n^4)-1]$, $e = [\delta_1(3l^4+6m^2n^2-1)+\delta_2(3m^4+6l^2n^2-1)+\delta_3(3n^4+6l^2m^2-1)]/6$, and $\delta_i = (D_i-D)/(D^2-L^2)^{1/2}$.

It has to be pointed out that factors A_i have been normalized ($A_1 + A_2 + A_3 + A_4 + A_5 = 1$).

Substitution of eq. (S10) into eq. (1) of the main text yields spectral density function for the model-free approach of anisotropically tumbling molecule

$$J^{MFA}(\omega) = \frac{2}{5}\sum_{i=1}^{5} A_i \left[\frac{S^2\tau_i}{1+(\omega\tau_i)^2} + \frac{(1-S^2)\tau_{\mathrm{int},i}}{1+(\omega\tau_{\mathrm{int},i})^2} \right] \qquad \text{(S11)}$$

where $1/\tau_{\mathrm{int},i} = 1/\tau_i + 1/\tau_{\mathrm{int}}$.

Similarly, substituting eq. (S10) into eq. (2) of the main text one obtains spectral density function for the extended model-free approach of anisotropically tumbling molecule

$$J^{EMFA}(\omega) = \frac{2}{5}\sum_{i=1}^{5} A_i \left[\frac{S_f^2 S_s^2 \tau_i}{1+(\omega\tau_i)^2} + \frac{(1-S_{f,i}^2)\tau_{f,i}}{1+(\omega\tau_{f,i})^2} + \frac{S_f^2(1-S_{s,i}^2)\tau_{s,i}}{1+(\omega\tau_{s,i})^2} \right] \qquad \text{(S12)}$$

where $1/\tau_{k,i} = 1/\tau_i + 1/\tau_{k,i}$. Indices *f* and *s* correspond to fast and slow internal motions.

Simplified extended model-free approach

Spectral density function in the formalism of extended model-free approach requires four parameters describing internal motions on two time scales: fast - *f* and slow - *s* besides parameter(s) characterizing diffusional tumbling. Each of internal motions is described by two parameters, generalized order parameters, S_f^2 and S_s^2 which correspond to the spatial freedom of the motions, and internal correlation time, $\tau_{int,f}$ and $\tau_{int,s}$. Almost all EMFA applications are limited to the use of simplified three-parameter spectral density function with $\tau_{int,f} = 0$. This model will be denoted as EMFA3. Then, the spectral density function takes shape

$$J^{EMFA3}(\omega) = \frac{2}{5} S_f^2 \left[\frac{S_s^2 \tau_R}{1+(\omega\tau_R)^2} + \frac{(1-S_s^2)\tau_s}{1+(\omega\tau_s)^2} \right] = S_f^2 J^{MFA}(\omega)$$

The expression given in square brackets is identical with the spectral density function of genuine model-free approach to an accuracy of the index. Substituting $J^{EMFA3}(\omega)$ to R_1 and R_2 formulae one obtains

$$R_1(J^{EMFA3}) = S_f^2 \left\{ R_{1,DD}(J^{MFA}) + R_{1,CSA}(J^{MFA}) \right\} = S_f^2 R_1(J^{MFA})$$

and

$$R_2(J^{EMFA3}) = S_f^2 \left\{ R_{2,DD}(J^{MFA}) + R_{2,CSA}(J^{MFA}) \right\} + R_{ex} = S_f^2 R_2(J^{MFA}) + (1-S_f^2) R_{ex}$$

Usually the term $(1-S_f^2)R_{ex}$ is negligible for the most frequent case of restricted mobility when S_f^2 is close to one. If not, the R_{ex} term can be unequivocally separated from R_2 owing to its square dependence on the magnetic field strength. Then both relaxation rates are scaled down by factor S_f^2 and this factor can be taken into account using genuine MFA spectral density functions and adequate choice of r_{NH} and $\Delta\sigma$ instead of EMFA3.

The third frequently measured relaxation parameter, *NOE*, is independent on S_f^2 scaling since

$$NOE(J^{EMFA3}) = 1 + \frac{\gamma_H}{\gamma_N} \frac{S_f^2 \sigma(J^{MFA})}{S_f^2 R_1(J^{MFA})} = NOE(J^{MFA})$$

Back calculated *NOE* values can be identical for use of $J^{MFA}(\omega)$ or $J^{EMFA3}(\omega)$.

Table S1. Comparison of experimental relaxation parameters with their back calculated values using MFA without {A} and with {B} *NOE* data[9] and EMFA3[9] and the result obtained in the present work {C} for Ile 18 and Leu 7 of SNase.[8]

Ile 18									
model	R_1@6.3 T	R_1@11.7 T	R_2@11.7 T	*NOE*@11.7 T	R_1@14.1 T	S^2	S_f^2, S_s^2	τ_{int} [ns]	Γ [a]
observed [b]	2.95±0.70	1.57±0.02	8.13±0.20	0.64±0.10	1.274±0.024	---	---	---	---
{A} MFA [c,d]	3.25	1.56	8.14	---	1.28	0.62	---	0.24	0.454
{B} MFA [c,e]	3.39	1.54	8.92	0.17	1.24	0.69	---	0.15	41.616
EMFA3 [c,f]	3.27	1.56	8.16	0.64	1.29	0.61	0.77; 0.80	1.8	0.661
{C} MFA [g,h]	3.39	1.58	8.13	0.62	1.26	0.77	---	0.06	0.675
Leu 7									
observed	2.65±0.38	1.62±0.06	7.35±0.27	0.46±0.10	1.351±0.011	---	---	---	---
{A} MFA [c,d]	3.15	1.61	7.30	-0.49	1.35	0.53	---	0.37	1.804
{B} MFA [c,e]	3.43	1.64	8.52	-0.15	1.35	0.65	---	0.31	60.025
EMFA3 [c,f]	3.12	1.59	7.31	0.47	1.35	0.53	0.78; 0.68	1.4	1.819
{C} MFA [h,i]	2.72	1.60	7.35	0.46	1.35	0.57	---	0.05	0.120

[a] target function Γ includes weighted deviations of 5 or 4 experimental data

[b] relaxation rates are reported in s^{-1}

[c] τ_R = 9.1 ns was determined separately from a global fit of the T_1/T_2 ratios; r_{NH} = 0.102 ns, $\Delta\sigma$ = –160 ppm (ref. 8)

[d] experimental *NOE* value excluded from optimization procedure

[e] experimental *NOE* value included into optimization procedure

[f] simplified EMFA3 with $\tau_f = 0$

[g] τ_R = 7.9 ns was determined from its simultaneous fit with local parameters of 56 residues

[h] r_{NH} = 0.104 nm[10] and $\Delta\sigma$ = –170 ppm[11-13] were applied in this calculation

[i] site specific τ_{mR} = 4.96 ns was determined from its simultaneous fit with remaining local parameters including exchange term

R_{ex} = 0.91 s^{-1} @ 6.3 T

Table S2

Partial target functions Γ_i and statistical tests for model selection of Thr 9 and Lys 11 residues of human ubiquitin calculated for relaxation data given in ref. 14. The more complicated model (EMFA) cannot be rejected if F value calculated using formula (A) given below is greater than tabulated F_{tabl}. For Akaike's Information Criteria (AIC) smaller value of the AIC given by formula (B) points out to the appropriate model.

$$F = \left[\frac{\Gamma(MFA) - \Gamma(EMFA)}{p(EMFA) - p(MFA)}\right] / \left[\frac{\Gamma(EMFA)}{N - p(EMFA)}\right] \qquad \text{(A)}$$

$$AIC(i) = N\ln\Gamma(i) + 2p(i) + 2p(i)[p(i)+1]/[N - p(i) - 1] \qquad \text{(B)}$$

In (A) and (B) formulae N is the number of experimental data and $p(i)$ - number of model parameters.

Data set [a]	Γ_i(MFA)	Γ_i(EMFA)	F	F_{tabl}@0.01	AIC(MFA)	AIC(EMFA)
(9) all data	39.272	3.085	23.46	18.0	43.84	40.14
(9) R_1, *NOE* rej. [b]	8.884	2.569	2.46	99.0	29.29	76.60
(11) all data	70.865	2.684	50.81	18.0	49.15	38.89
(11) R_1, *NOE* rej. [b]	30.274	1.320	21.94	99.0	37.87	71.94

[a] (9) denotes Thr 9 and (11) denotes Lys 11

[b] Rejection of R_1 and *NOE* at 14.1 T

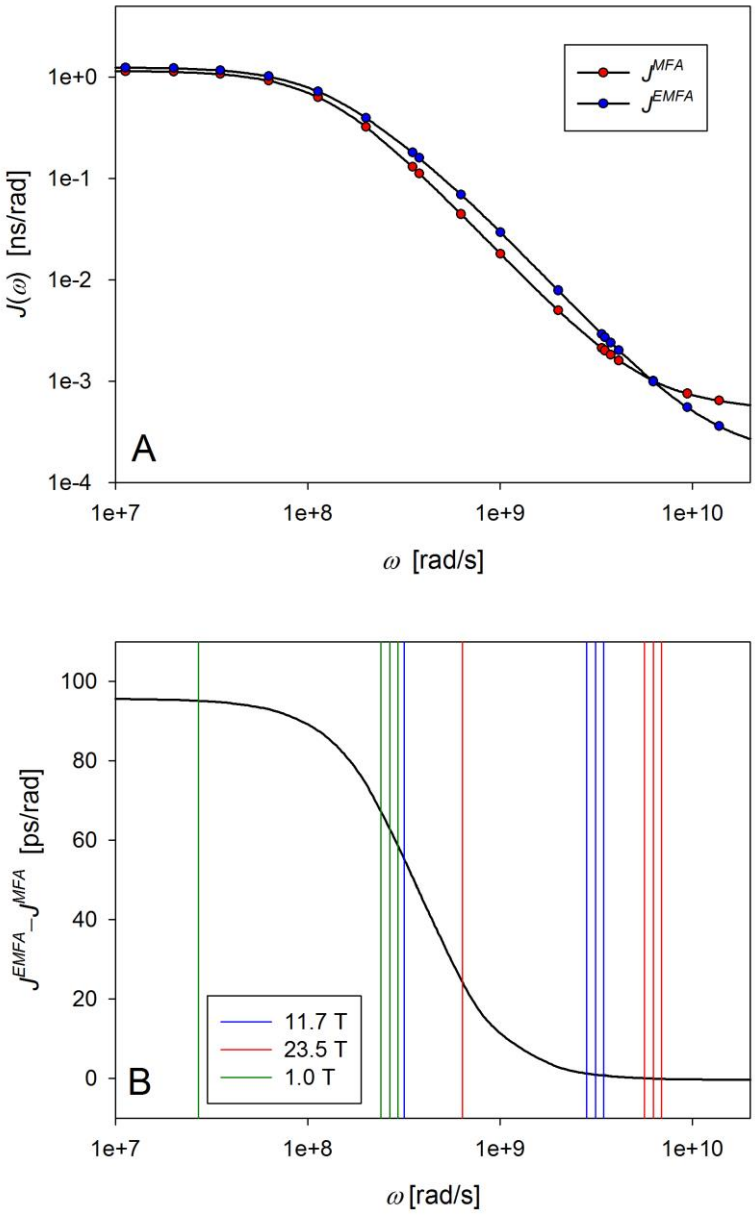

Figure S1

A) Dependence of the spectral densities, $J(\omega)$, for two free-approach models, MFA and EMFA. Calculations were performed for τ_R = 8 ns, S^2_{MFA} = 0.72, $S^2_{f,EMFA}$ = 0.9, $S^2_{s,EMFA}$ = 0.8, $\tau_{int,MFA}$ = $\tau_{int,f,EMFA}$ = 10 ps, $\tau_{int,s,EMFA}$ = 4 ns. **B**) Difference between spectral density functions presented in part **A**. Frequencies sampled by the most often measured relaxation data R_1, R_2, and *NOE* at three magnetic field strengths are marked by vertical lines. Fifth sampled frequency $\omega = 0$ is outside of the plotted range. Inflection point of the difference curve appears at $\omega = 1/\tau_s = (\tau_R + \tau_{int,s})/\tau_R\tau_{\mathrm{int},s}$.

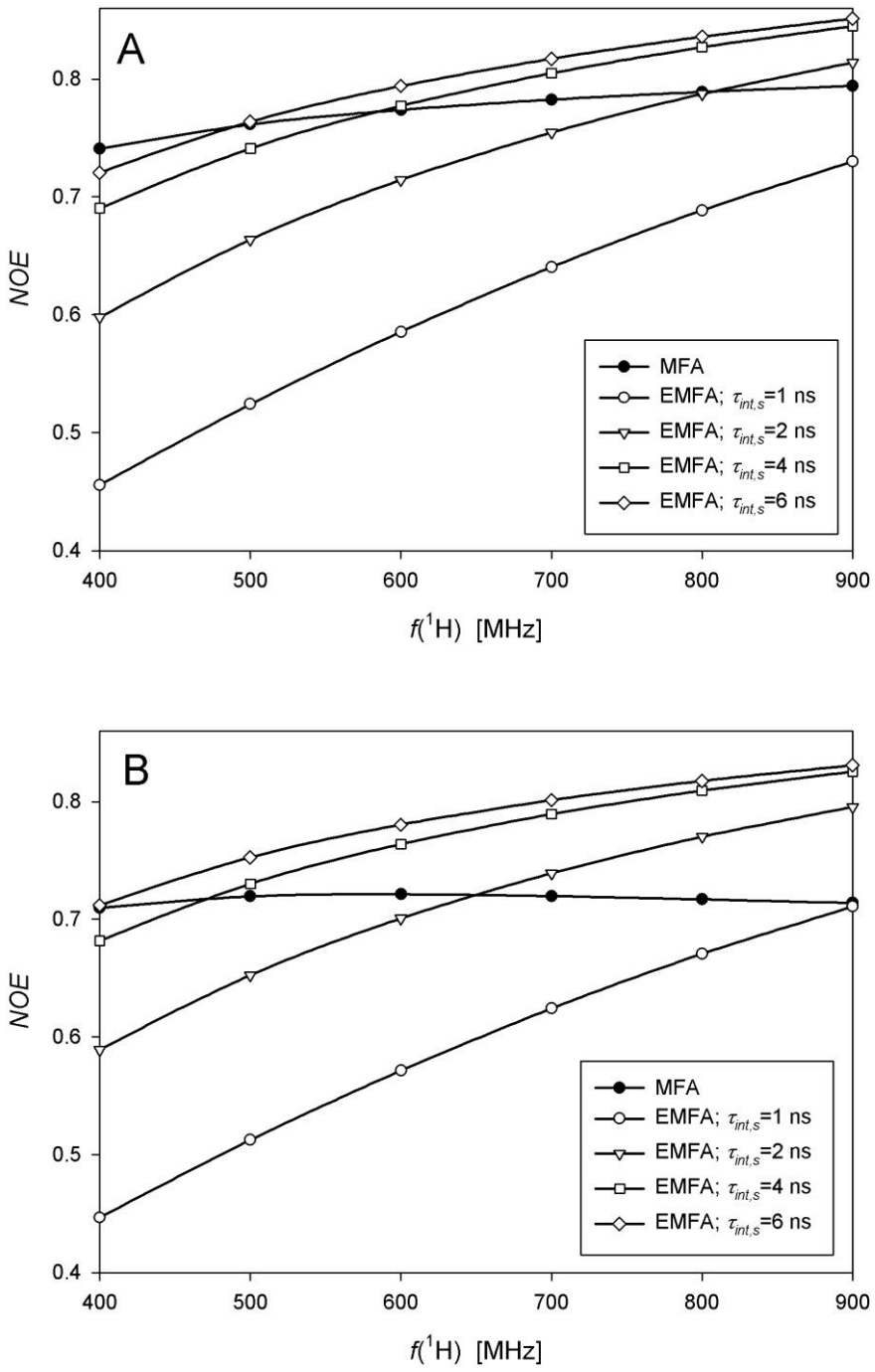

Figure S2

NOE values vs. basic frequency of NMR spectrometer calculated for MFA and EMFA assuming variable $\tau_{int,s}$ (see legends) and $\tau_{int,f}$ values (A: $\tau_{int,f}$ = 10 ps; B: $\tau_{int,f}$ = 20 ps). Remaining model parameters were the same as given in the legend to Fig. S1.

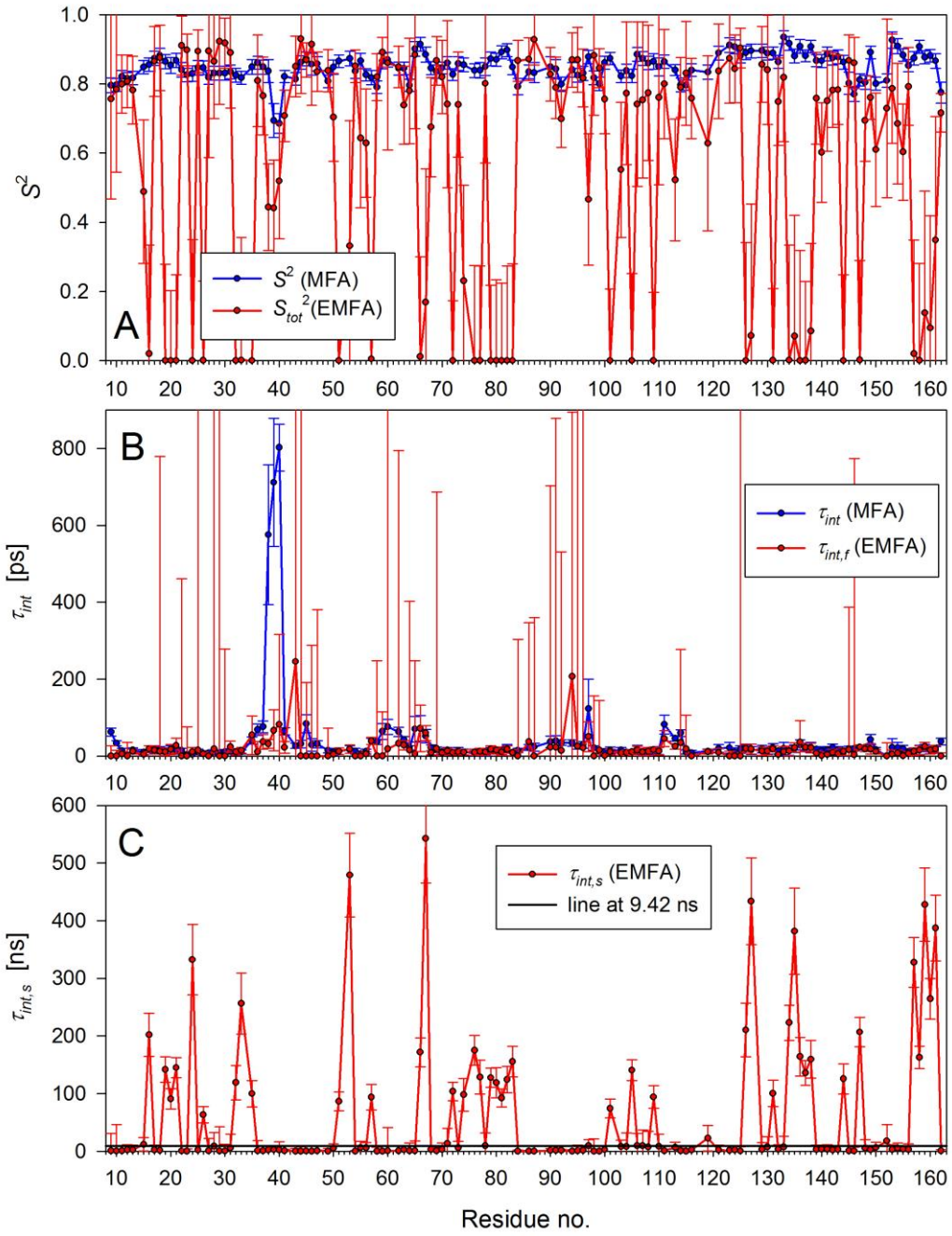

Figure S3

Residue specific values of the generalized order parameters and correlation times of internal motions obtained in MFA and EMFA calculations for ^{15}N relaxation data of olfactory marker protein.[15] (A) comparison of S^2(MFA) and S_{tot}^2(EMFA) is irrelevant, (B) τ_{int}(MFA) and $\tau_{int,f}$(EMFA) values do not correspond one another, (C) horizontal black line represents $\langle \tau_R \rangle = 9.42$ ns; $\tau_{int,s}$(EMFA) exceeding $\langle \tau_R \rangle$ are senseless in the light of data presented in Figs. 6 and 8 as well as analysis presented in section 7.

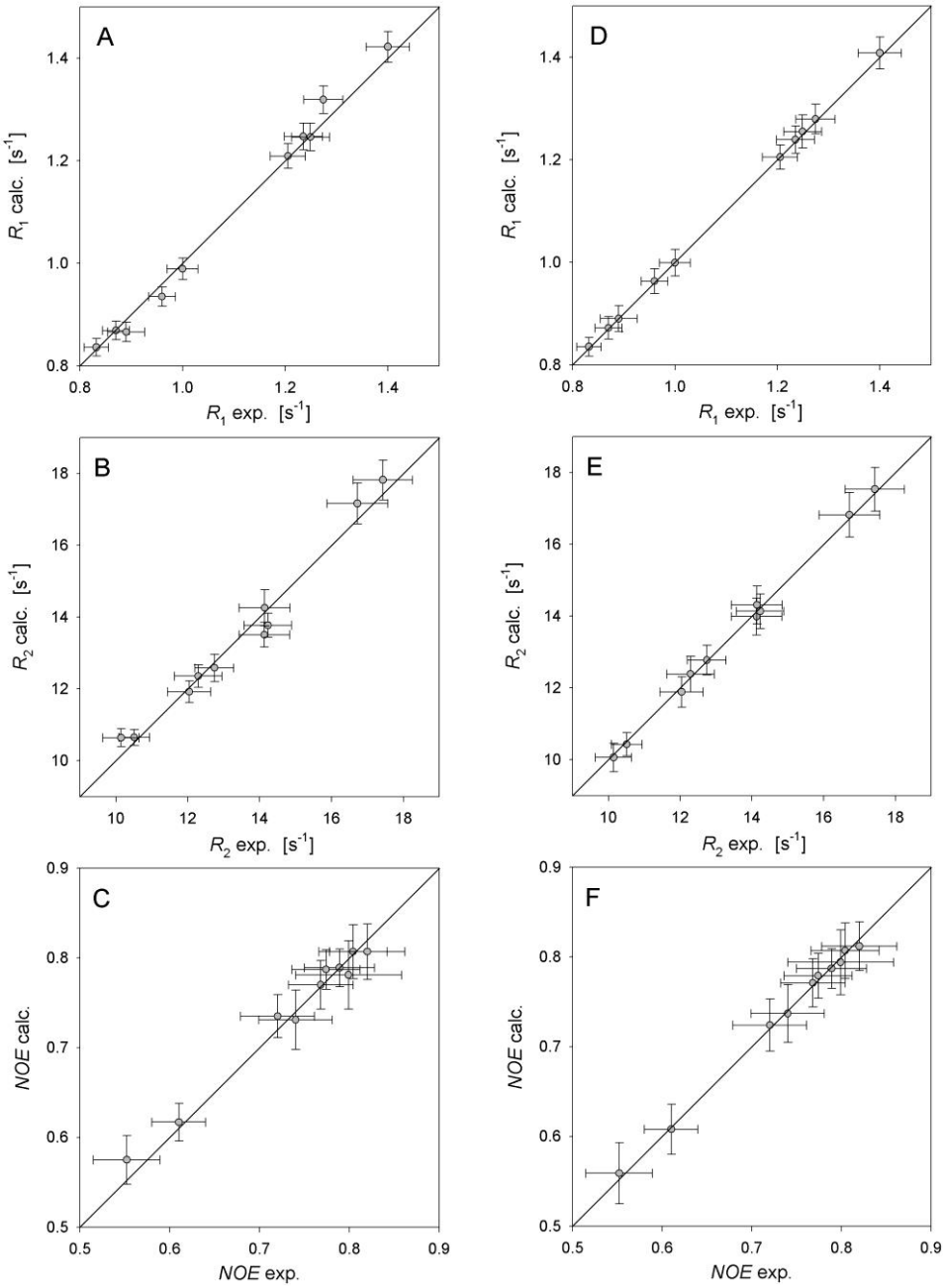

Figure S4

Left hand side figures show correlations between experimental and the MFA back calculated values of R_1 (A), R_2 (B), and *NOE* (C) values for five OMP residues (Arg 28, Asp 41, Met 95, Ala 103, and Leu 123). $\Sigma\Gamma_i$(MFA) = 7.50. Correlation coefficients r^2 are equal to 0.99, 0.98, and 0.99 for R_1, R_2, and *NOE* plots, respectively. Right hand side figures show corresponding correlations between experimental and the EMFA back calculated values of R_1 (D), R_2 (E), and *NOE* (F) values. $\Sigma\Gamma_i$(EMFA) = 0.04.

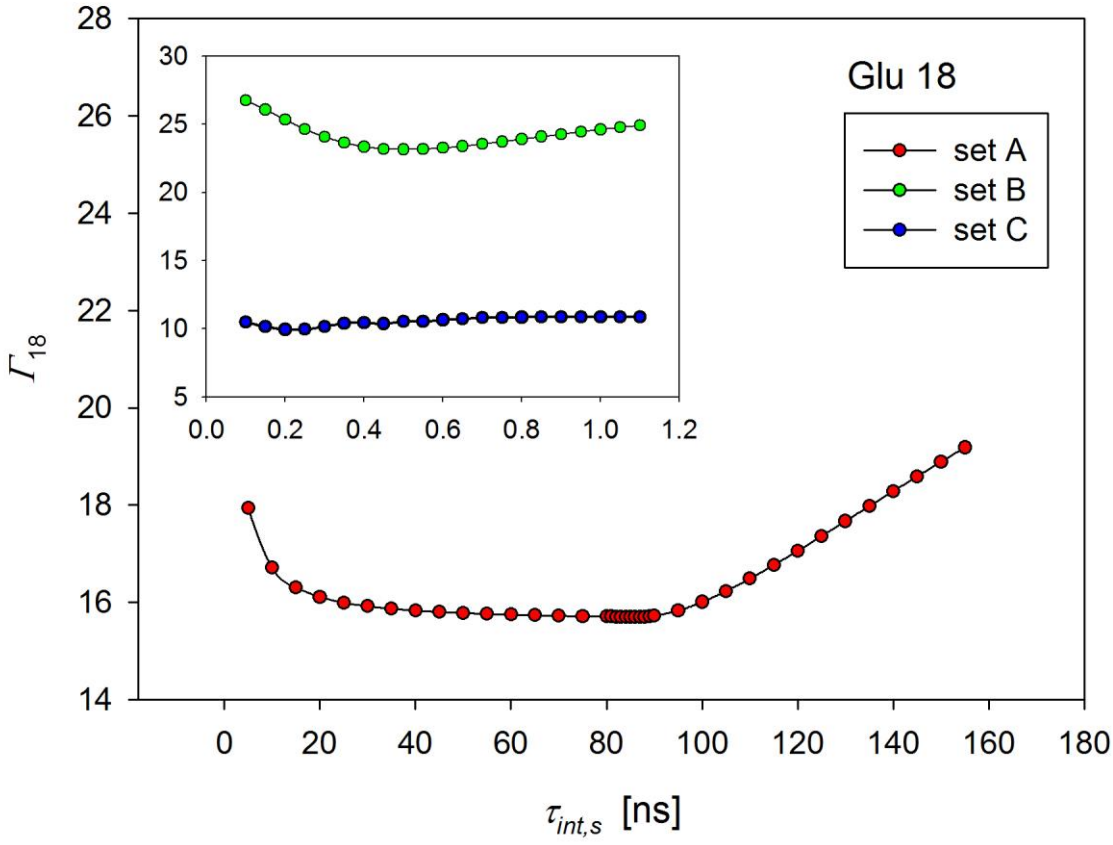

Figure S5

Profiles of partial target function $\Gamma(\tau_{int,s})$ for Glu 18 of human ubiquitin derived from the relaxation data published in refs. 16 (set A), 14 (set B), and 17 (set C). $\Gamma(\tau_s)$ minima were found at 86.7 ns (set A), 0.51 ns (set B) and 0.22 ns (set C). Averaged overall correlation times $\langle \tau_R \rangle$ are 5.05, 4.93, and 4.56 ns for set A, B, and C, respectively.

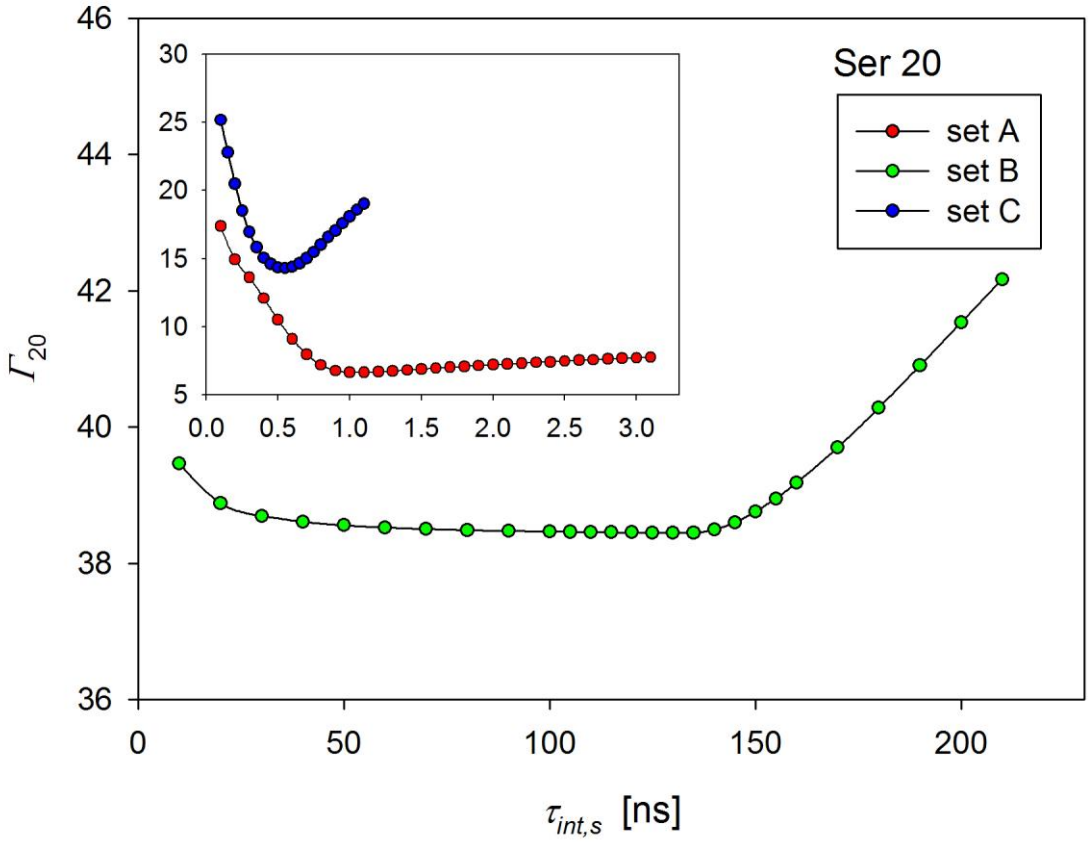

Figure S6

Profiles of partial target function $\Gamma(\tau_{int,s})$ for Ser 20 of human ubiquitin derived from the relaxation data published in refs. 16 (set A), 14 (set B), and 17 (set C). $\Gamma(\tau_s)$ minima were found at 1.1 ns (set A), 134 ns (set B), and 0.53 ns (set C). Averaged overall correlation times $\langle\tau_R\rangle$ are 5.05, 4.93, and 4.56 ns for set A, B, and C, respectively.

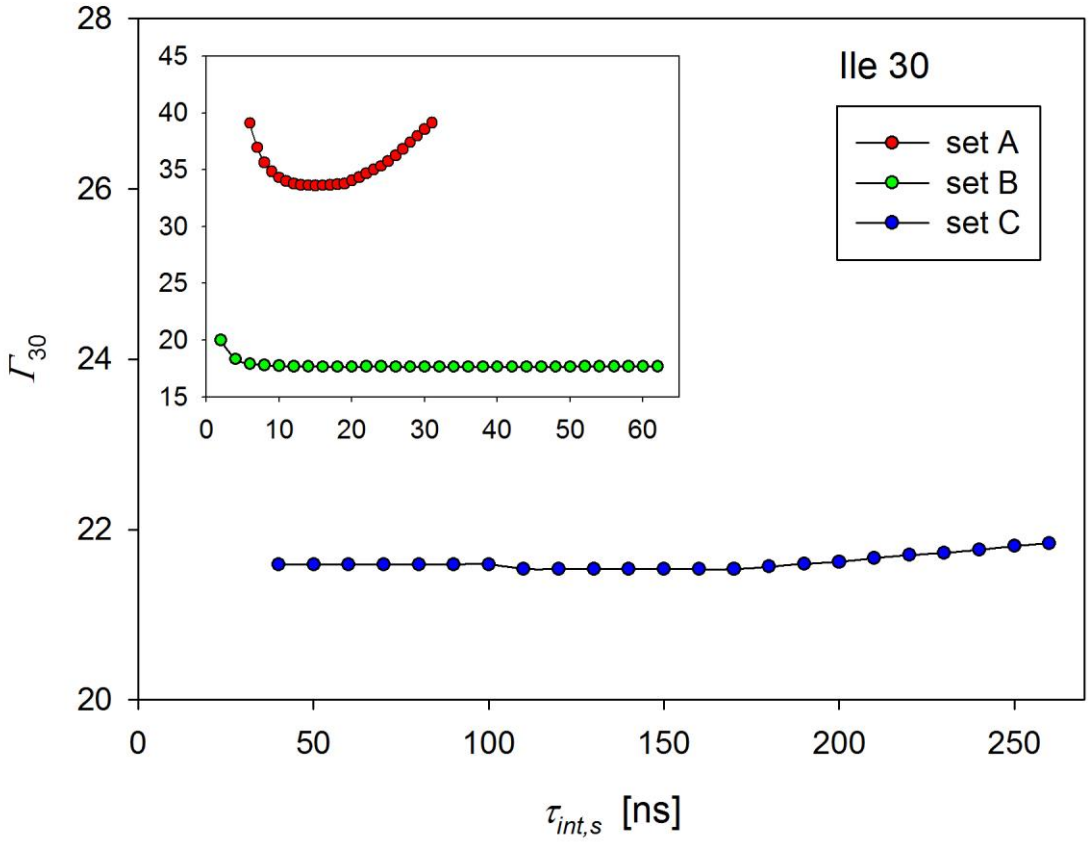

Figure S7

Profiles of partial target function $\Gamma(\tau_{int,s})$ for Ile 30 of human ubiquitin derived from the relaxation data published in refs. 16 (set A), 14 (set B), and 17 (set C). $\Gamma(\tau_s)$ minima were found at 14.84 ns (set A), 29.30 ns (set B) and 150.00 ns (set C). Averaged overall correlation times $\langle \tau_R \rangle$ are 5.05, 4.93, and 4.56 ns for set A, B, and C, respectively.

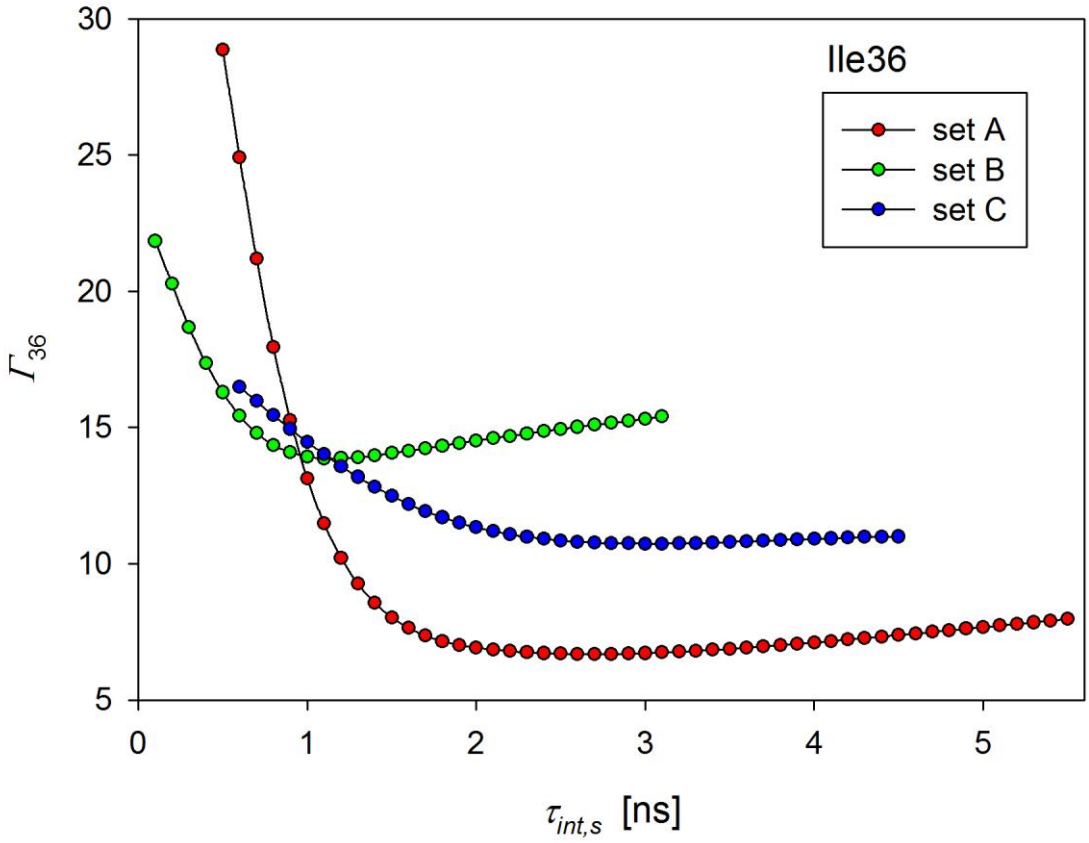

Figure S8

Profiles of partial target function $\Gamma(\tau_{int,s})$ for Ile 36 of human ubiquitin derived from the relaxation data published in refs. 16 (set A), 14 (set B), and 17 (set C). $\Gamma(\tau_s)$ minima were found at 2.62 ns (set A), 1.15 ns (set B) and 3.05 ns (set C). Averaged overall correlation times $\langle\tau_R\rangle$ are 5.05, 4.93, and 4.56 ns for set A, B, and C, respectively.

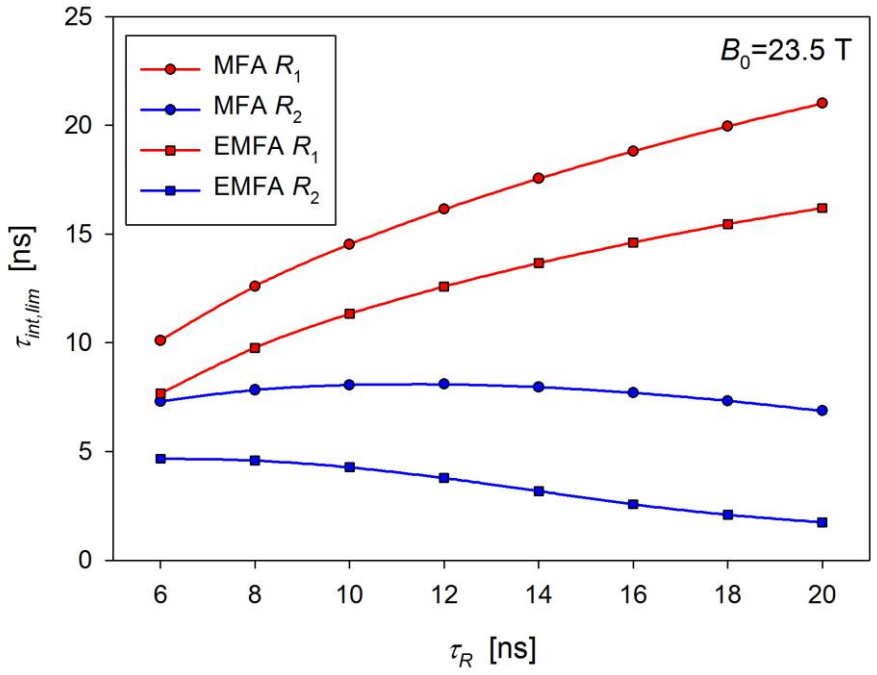

Figure S9

The boundary values of $\tau_{int,lim}$ determined from the normalized derivatives of relaxation rates R_1 (red) and R_2 (blue) vs. rotational correlation time τ_R at 23.5 T. Relaxation rates were calculated for MFA (circles) assuming the following input parameter $S^2 = 0.70$, and for EMFA with parameters: $\tau_R = 8$ ns, $S_f^2 = 0.90$, $S_s^2 = 0.80$, $\tau_{int,f} = 100$ ps. For both models $r_{NH} = 0.104$ nm, and $\Delta\sigma = -170$ ppm.

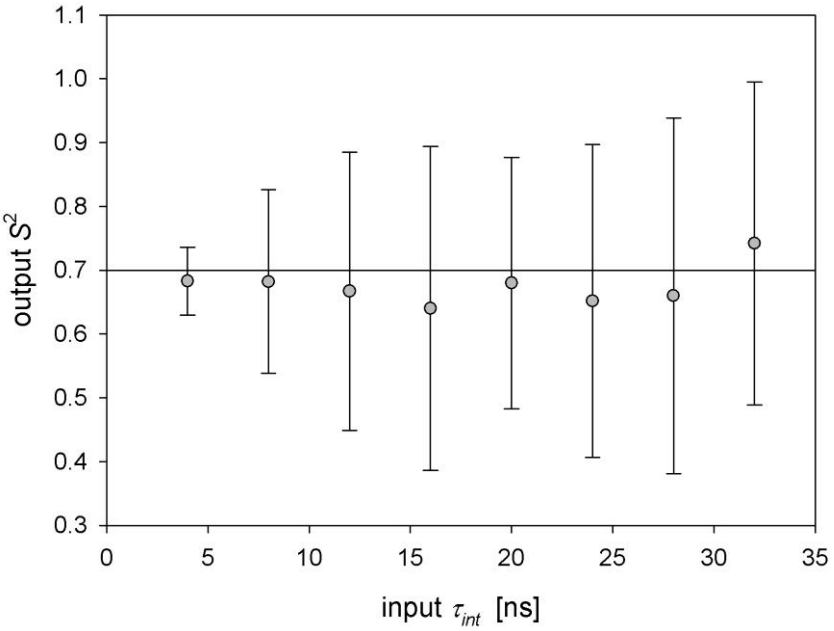

Figure S10

Reproducibility of S^2 parameter. True input data were calculated in the frame of MFA for τ_R = 8 ns, S^2 = 0.70, r_{NH} = 0.104 nm, and $\Delta\sigma$ = –170 ppm at three magnetic fields 16.4, 18.8, and 21.1 T. Assumed data accuracies were set to $\Delta R_i/R_i$ = 0.01 and $\Delta NOE/NOE$ = 0.05. Mean values of output S^2 and their standard deviations derived in the minimization of target function χ were obtained from 1000 Monte Carlo simulations.

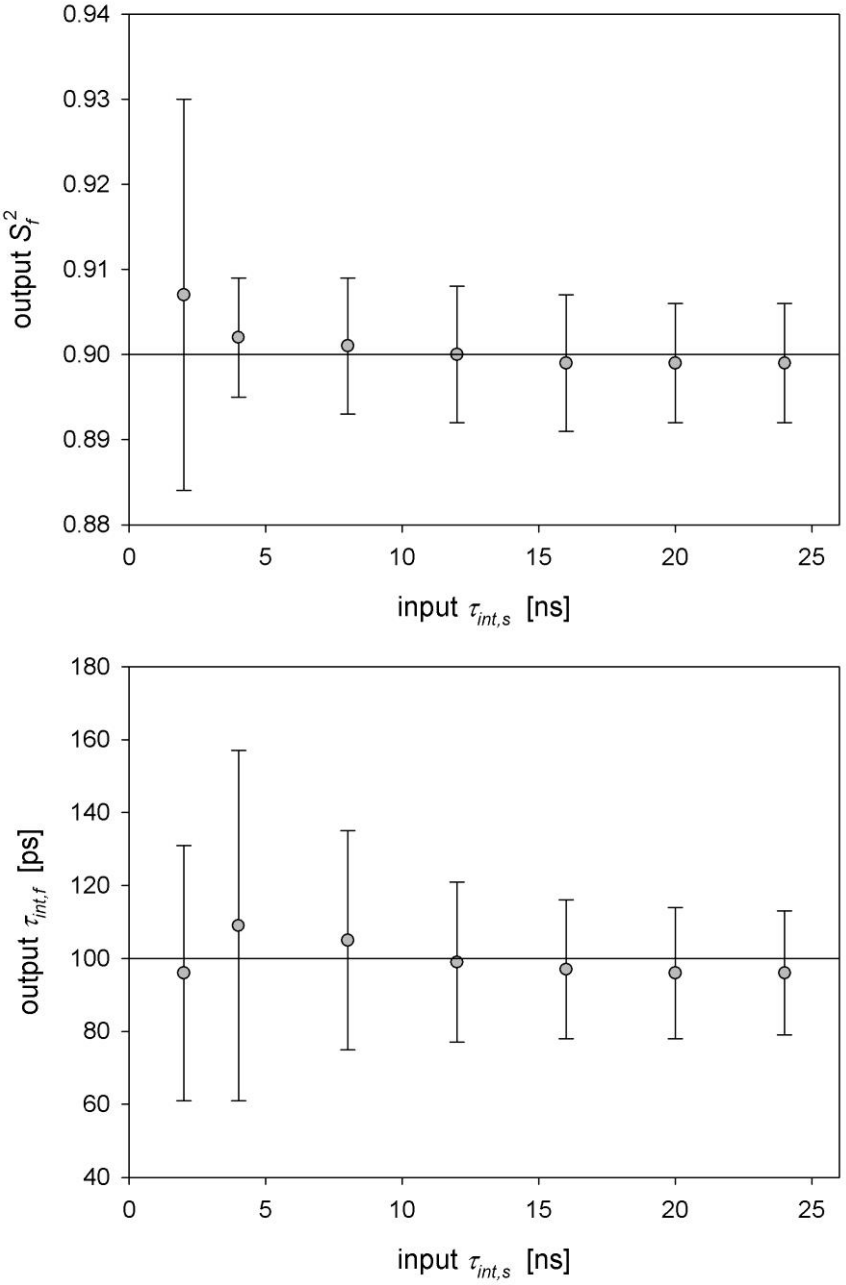

Figure S11

Reproducibility of S_f^2 and $\tau_{int,f}$ parameters. True input data were calculated in the frame of EMFA for τ_R = 8 ns, S_f^2 = 0.90, S_s^2 = 0.80, $\tau_{int,f}$ = 100 ps, r_{NH} = 0.104 nm, and $\Delta\sigma$ = –170 ppm at three magnetic fields 16.4, 18.8, and 21.1 T. Assumed data accuracies were set to $\Delta R_i/R_i$ = 0.01 and $\Delta NOE/NOE$ = 0.05. Mean values of output parameters and their standard deviations derived in the minimization of target function χ were obtained from 1000 Monte Carlo simulations.

References

(1) Boyd, J.; Hommel, U.; Campbell, I. D. Influence of Cross-Corrleation Between Dipolar and Anisotropic Chemical Shift Relaxation Mechanisms Upon Longitudinal Relaxation Rates of ^{15}N In Macromolecules. *Chem. Phys. Lett*. **1990**, *175*, 477−482.

(2) Kay, L. E.; Nicholson, L. K.; Delaglio, F.; Bax, A.; Torchia, D. A. Pulse Sequences for Removal of the Effects of Cross-Correlation Between Dipolar and Chemical-Shift Anisotropy Relaxation Mechanism on the Measurement Of Heteronuclear T1 And T2 Values In Proteins. *J. Magn. Reson*. **1992**, *79*, 359−375.

(3) Abragam, A. *The Principles of Nuclear Magnetism*; Oxford University Press: London, U.K., 1961.

(4) Stone, M. J.; Fairbrother, W. J.; Palmer, III, A. G.; Reizer, J.; Saier, Jr., M. H.; Wright, P. E. Backbone Dynamics of the Bacillus Subtilis Glucose Permease IIA Domain Determined from Nitrogen-15N NMR Relaxation Measurements. *Biochemistry* **1992**, *31*, 4394−4406.

(5) Frahm, J. Multiple-pulse FT-NMR Experiments for Kinetic Applications. *J. Magn. Reson*. **1982**, *47*, 209−228.

(6) Davis, D. G.; Perlman, M. E.; London, R. E. Direct Measurements of the Dissociation-Rate Constant for Inhibitor-Enzyme Complexes via the $T_{1\rho}$ and T_2 (CPMG) Methods. *J. Magn. Reson*. **1994**, *B104*, 266−275.

(7) Woessner, D. E. Nuclear Spin Relaxation in Ellipsoid Undergoing Rotational Brownian Motion. *J. Chem. Phys*. **1962**, *37*, 647−654.

(8) Kay, L. E.; Torchia, D. A.; Bax, A. Backbone Dynamics of Proteins as Studied By ^{15}N Inverse Detected Heteronuclear NMR Spectroscopy: Application to Staphylococcal Nuclease. *Biochemistry* **1989**, *28*, 8972−8979.

(9) Clore, G. M.; Szabo, A.; Bax, A.; Kay, L. E.; Driscoll, P. C.; Gronenborn, A. M. Deviations from the Simple Two-Parameter Model-Free Approach to the Interpretation of Nitrogen-15 Muclear Magnetic Relaxation of Proteins. *J. Am. Chem. Soc*. **1990**, *112*, 4989−4991.

(10) Ottinger, M.; Bax, A. Characterization of Magnetically Oriented Phospholipid Micelles for Measurement of Dipolar Couplings in Macromolecules. *J. Am. Chem. Soc.* **1998**, *120*, 12334−12341.

(11) Tjandra, N.; Wingfield, P.; Stahl, S.; Bax, A. Anisotropic Rotational Diffusion of Perdeuterated HIV Protease From 15N NMR Relaxation Studies at Two Fields. *J. Biomol. NMR* **1996**, *8*, 273–284.

(12) Pandey, M. K.; Vivekanandan, S.; Ahuja, S.; Pichumani, K.; Im, S-C.; Waskell, L.; Ramamoorthy, A. Determination on 15N Chemical Shift Anisotropy from a Membrane-Bound Protein by NMR Spectroscopy *J. Phys. Chem. B* **2012**, *116*, 7181−7189.

(13) Kroenke, C. D.; Rance, M.; Palmer III, A. G. Variability oft he 15N Chemical Shift Anisotropy in Escherichia Coli Ribonuclease H in Solution. *J. Am. Chem. Soc.* **1999**, *121***,** 10119−10125.

(14) Charlier, C.; Nawaz Khan, S.; Marquardsen, T.; Pelupessy, P.; Sakellariou, D.; Reiss, V.; Bodenhausen, G.; Engelke, F.; Ferrage, F. Nanosecond Time Scale Motions in Proteins Revealed by High-Resolution NMR Relaxometry. *J. Am. Chem. Soc*. **2013**, *135*, 18665−18672.

(15) Gitti, R. K.; Wright, N. T.; Margolis, J. W.; Varney, K. M.; Weber, D. J.; Margolis, F. L. Backbone Dynamics of the Olfactory Marker Protein As Studied by ^{15}N NMR Relaxation Measurements. *Biochemistry* **2005**, *44***,** 9673–9679.

(16) Damberg, P.; Jarvet, J.; Gräslund, A. Limited Variations in 15N CSA Magnitudes and Orientations in Ubiquitin Are Revealed by Joint Analysis of Longitudinal and Transverse NMR Relaxation. *J. Am. Chem. Soc*. **2005**, *127*, 1995–2005.

(17) Lee, A. L.; Wand, A. J. Assesing Potential Bias in the Determination of Rotational Correlation Times of Proteins by Nmr Relaxation. *J. Biomol. NMR* **1999**, *13*, 101–112.